International Journal of Applied Engineering Research ISSN 0973-4562 Volume 10, Number 18 (2015) pp 39735-39744

Experimental and Numerical Analysis of Air Preheater for Waste Heat Recovery of CI Engine using different fin type

P. P. Patnaik

Phd Scholar, Department of Mechanical Engineering, S 'O' A University, Khandagiri, Bhubaneswar-30, Odisha
ppatnaik9@gmail.com

S.K.Acharya

Associate Professor, Department of Mechanical Engineering S 'O' A University, Khandagiri Bhubaneswar-30, Odisha
saroj.acharya76@gmail.com

H.C.Das

Professor, Department of Mechanical Engineering, S 'O' A University, Khandagiri, Bhubaneswar-30, Odisha
harishdas@soauniversity.ac.in

MD.AYUB Ansari

PG Scholar, Department of Mechanical Engineering S 'O' A University, Khandagiri Bhubaneswar-30, Odisha
mdayubansari2014@gmail.com

Abstract
The simulation of waste heat of exhaust gas recovered by heat exchanger (finned type) using rectangular and triangular fins which is intended for increasing the efficiency of engine by preheating the air taken for diesel engine is explored in this paper. Solid Works is used for generating geometric model and meshed by using ANSYS Mesh tool. The heat exchanger is modeled numerically, using k-ε viscous realizable and RNG model and numerical simulation of heat exchanger was analyzed by using a three dimensional numerical computation technique. The results of this study shows triangular fins give maximum heat recovery as compared to rectangular fin. The CFD results and experimental results are validated intending to a close value. Using preheated air in cold weather condition brake thermal efficiency increases and brake specific fuel consumption decreases with increase in load. Carbon monoxide (CO) and hydrocarbon (HC) emissions are reduced and nitrogen oxide (NO) emission increased during air pre-heating as compared to cold weather condition.

Keywords: Finned heat exchanger, Computational Fluid Dynamics (CFD), ANSYS, air preheating

Introduction

Each form of energy is valuable in this modern world where energy plays a vital role as the world is at a stage of energy crisis. A large amount of energy goes as waste from the exhausts of engine, which is about 30 – 40% of fuel energy and only 10 – 30% of fuel energy is converted to useful work [1-4]. Diesel engine exhaust gas can be a vital source in order to have excess power using an additional rankine cycle. Water is used as a working fluid to quantify the exhaust heat by using two heat exchangers so that 16% excess power was found. After optimizing the pressure of working fluid and position of the heat exchanger, power was enhanced by 7.7% [5]. Quiwang Wang et al. [6] experimentally conducted heat transformer performance has been improved by the combination of heat exchangers (CMSP-STHX) with helical baffles in outer shell. With the help of CFD method, the CMSP-STHX has been compared with shell and tube heat exchanger. Bostjan Dobronic et al. [7] believed that the air pre-heaters believed that overall efficiency can be improved negotiable by the help of air pre heaters.Three dimensional numerical model and fluid dynamics were used for the analysis of a rotary pre heater. Experimental results and numerical analysis have dependency on flue gas parameters. They proposed a method based on the results for online monitoring of the tightness of the radial seals. Air pre heater is one of key components in today's energy-saving technology. M.Zeng et al. [8] experimentally investigated the characteristics i.e, heat transfer and pressure drop of a plate fin structure under different condition. Design and development of pre heater can be improvised from this study. Ting Ma et al. [9] presented the performance of heat transfer in the ribbed channel of heat exchanger. The inside temperature ranges from 850k to 1250k and the ratio between channel height to rib height varies from 12.04 to 3.The results shows the improvement of the heat transfer due to increase in height of rib. The heat transfer and temperature distribution equations for circular convective radioactive porous fins are presented. It's assumed that the thickness of circular fins varies with radius so four different shapes, rectangular, convex, triangular and exponential, are considered [10]. The effect of spacing, height, thickness and material of fin on pressure drop and heat transfer were determined by using CFD software ANSYS FLUENT. It was evident from the experiment that heat transfer is directly proportional to fin

height [11]. Juan Li et.al [12] proposed the theory of studying convective heat transfer and fluid flow characteristic of the triangular perforated fin with numerical simulation. The secondary flows and vertices can improve the synergy between the velocity and temperature -gradient, which is the cause why triangular perforated fin enhances the heat transfer. M.Turkyilmazoglu et.al [13] studied the effects of fin efficiency and the enhancement of heat transfer when the fins are subjected to stretching and shrinking in the direction of motion. Selecting different parameters like the Peclet number, Shrinking/Stretching parameter, sink temperature parameter etc; comparison was made for the efficiency of stretched and non-stretched longitudinal fins. The result shows that the efficiency of the shrinking fins is comparatively more than that of the stretching fins. For the cross-corrugated triangular ducts, both the flow and the heat and mass transfer demonstrate cyclic patterns. At the entrance region, the cyclic mean values of friction factor, Nusselt and Sherwood numbers decrease rapidly along the flow. Compared to parallel-plate or plate-fin structures with common composite membrane materials, the cross-corrugated structure with one-step made asymmetric membranes would have a 20% higher sensible effectiveness, a 40% higher latent effectiveness, with about 4 times higher pressure drop penalty [14]. In some applications it may be required to have unidirectional heat transfer from a medium to a secondary medium with temperature swings above and below the temperature of the medium from which heat is to be discharged (transferred). While the hot and cold streams must be in direct contact in a conventional HX, a HPHX can transfer heat between two media located remotely from each other, promoting considerable design flexibility [15]. Mushtaq Ismail Hasan [16] investigated the micro pin fin heat sink numerically with three geometries (square, circular, triangular) with unfinned micro channel hear sink. The fins arranged here are in a staggered configuration because of better heat transfer than the inline configuration. The model was solved with pure water as cooling fluid with constant properties then was repeated for nanofluid with different fin geometries. The results that were found were using of nanofluid as coolant with all fin geometries leads to enhanced cooling process. Heat transfer rate and pressure drop increases with increasing the volumetric concentration of nano fluid and heat transfer rate of circular fins is higher than any other fins with square fins causing maximum pressure drop. Tin Ma et.al [17] illustrated the effects of inlet temperature and rib height on the fluid flow and heat transfer performances of the ribbed channel inside the high temperature heat exchanger. The results shows that increased the rib height results in enhancement the flow disturbance which improves the heat transfer performance.

Experimental Procedure

The engine selected for the testing is 4 stroke, 3.5 kW, compression ratio of 18, water cooled and direct injection diesel engine of Kirloskar make at a rated speed of 1500 rpm. To preheat the inlet air, an air preheater is used to exchange heat between exhaust gas and fresh inlet air as shown in Fig.1. Hot air comes out of an air preheater is supplied to the inlet of the engine for combustion. Rectangular and triangular fins are provided over the exhaust pipe for better heat transfer. Preheating of the engine inlet air by waste exhaust gas energy was considered to improve the performance of the engine. Air pre-heater was designed and fabricated basing on the principle that, heat rejected by the exhaust gas in air pre-heater is equal to the heat absorbed by the circulating air. To enhance the rate of heat transfer from exhaust gas to air, rectangular and triangular fins are used. Air pre heater has an air inlet which is connected to air box and outlet which is connected to engine. Thermocouples were connected to measure the exhaust gas temperature and fresh air temperatures at the inlet and outlet. Temperature of the fresh air is controlled by closing and opening of the control valve in the exhaust line at the inlet side. The preheated air with temperature around 40°C was directly allowed to enter into the engine cylinder through inlet pipe connected form air preheater outlet to engine inlet. Air pre-heater is also known as finned type heat exchanger. The exhaust gas emissions were measured by online AVL-444 model multi gas analyzer. Multi gas analyzer is capable of measuring CO (0 to 10% vol), HC (0 to 20000ppm), CO_2 (0 to 20% vol) and NO (0 to 5000ppm) compositions of the exhaust gas. Smoke opacity is measured with AVL-437 model smoke meter (measuring range 0 to100%).

Fig.1 Actual Experimental Setup.

In this paper, the heat exchanger is modeled and analyzed numerically, using k-ε viscous realizable and RNG model. The main goal of the study is to recover waste engine heat and utilizing it to improve the engine performance during cold weather condition by preheating the inlet air.

Numerical Modelling

The numerical modelling was done using a three dimensional steady-state turbulent flow system. As we have considered a steady-state model the time dependent factors were not considered. The equations are as follows:

Continuity Equation:

$$\nabla . (\rho \vec{V}) = 0 \quad (1)$$

Momentum Equations:

X-momentum:

$$\nabla.(\rho u\vec{V}) = -\frac{\partial p}{\partial x} + \frac{\partial \tau_{xx}}{\partial x} + \frac{\partial \tau_{yx}}{\partial y} + \frac{\partial \tau_{zx}}{\partial z} \quad (2)$$

Y-momentum:

$$\nabla.(\rho v\vec{V}) = -\frac{\partial p}{\partial y} + \frac{\partial \tau_{xy}}{\partial x} + \frac{\partial \tau_{yy}}{\partial y} + \frac{\partial \tau_{zy}}{\partial z} + \rho g \quad (3)$$

Z-momentum:

$$\nabla.(\rho w\vec{V}) = -\frac{\partial p}{\partial z} + \frac{\partial \tau_{xz}}{\partial x} + \frac{\partial \tau_{yz}}{\partial y} + \frac{\partial \tau_{zz}}{\partial z} \quad (4)$$

Energy equation

$$\rho c_p\left(u\frac{\partial T}{\partial x} + v\frac{\partial T}{\partial y} + w\frac{\partial T}{\partial z}\right) = \lambda\left(\frac{\partial^2 T}{\partial x^2} + \frac{\partial^2 T}{\partial y^2} + \frac{\partial^2 T}{\partial z^2}\right) \quad (5)$$

In this paper one of the viscous models was examined. i.e Realizable k-ε model.

$$\frac{\partial}{\partial t}(\rho k) + \frac{\partial}{\partial x_j}(\rho k u_j) = \frac{\partial}{\partial x_j}\left[\left(\mu + \frac{\mu_t}{\sigma_k}\right)\frac{\partial k}{\partial x_j}\right] + G_k + G_b - \rho\varepsilon - Y_M + S_k \quad (6)$$

and

$$\frac{\partial}{\partial t}(\rho\varepsilon) + \frac{\partial}{\partial x_j}(\rho\varepsilon u_j) = \frac{\partial}{\partial x_j}\left[\left(\mu + \frac{\mu_t}{\sigma_\varepsilon}\right)\frac{\partial \varepsilon}{\partial x_j}\right] + \rho C_1 S\varepsilon - \rho C_2\frac{\varepsilon^2}{k+\sqrt{v\varepsilon}} + C_{1\varepsilon}\frac{\varepsilon}{k}C_{3\varepsilon}G_b + S_\varepsilon \quad (7)$$

And the other one being RNG k-ε model.

$$\frac{\partial}{\partial t}(\rho k) + \frac{\partial}{\partial x_i}(\rho k u_i) = \frac{\partial}{\partial x_j}\left[\alpha_k \mu_{eff}\frac{\partial k}{\partial x_j}\right] + G_k + G_b - \rho\varepsilon - Y_M + S_k \quad (8)$$

and

$$\frac{\partial}{\partial t}(\rho\varepsilon) + \frac{\partial}{\partial x_i}(\rho\varepsilon u_i) = \frac{\partial}{\partial x_j}\left[\alpha_\varepsilon \mu_{eff}\frac{\partial \varepsilon}{\partial x_j}\right] + C_{1\varepsilon}\frac{\varepsilon}{K}(G_k + C_{3\varepsilon}G_b) - \rho C_{2\varepsilon}\frac{\varepsilon^2}{k} - R_\varepsilon + S_\varepsilon \quad (9)$$

Where,

$$C_1 = max\left[0.43, \frac{\eta}{\eta+5}\right], \eta = S\frac{k}{\varepsilon}, S = \sqrt{2S_{ij}S_{ij}}$$

G_k is the generation of turbulent kinetic energy

G_b is the kinetic energy is due to buoyancy

C_2 and $C_1\varepsilon$ are constants

σ_k and σ_ε are the turbulent Prandtl numbers for k and ε respectively

S_k and S_ε are the user defined source terms

Y_M represents the contribution of the fluctuating dilatation in compressible turbulence to the overall dissipation rate.

Modeling

In this study, geometric model was generated using Solid Works and the dimensions are mentioned below in the Table 1. The sectional view of fins is shown in Fig 2, the full sectional view is shown in Fig 3 but Fig 4 and Fig 5 shows the transparent model and original full views of HEX. Thermal properties of mild steel, air and exhaust gases are shown in Table 2. Then the model was meshed using meshing module in ansys. There are 904039 number of elements and 295843 number of nodes.

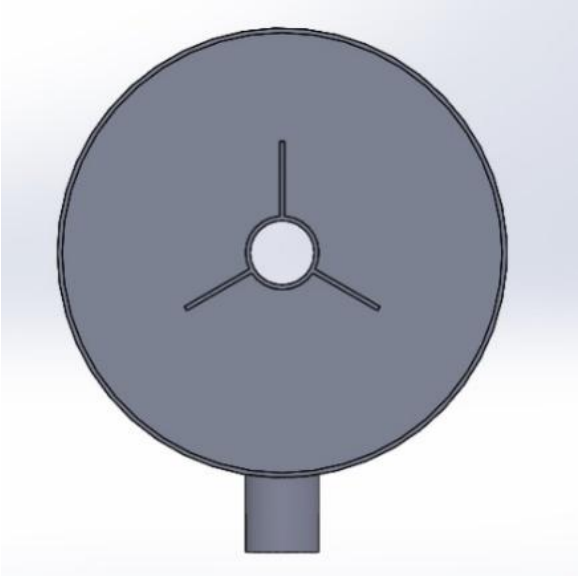

Fig.2. Recharging Framework

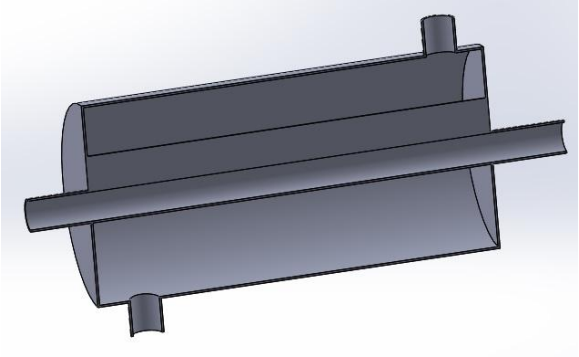

Fig 3. Full section view of heat exchanger

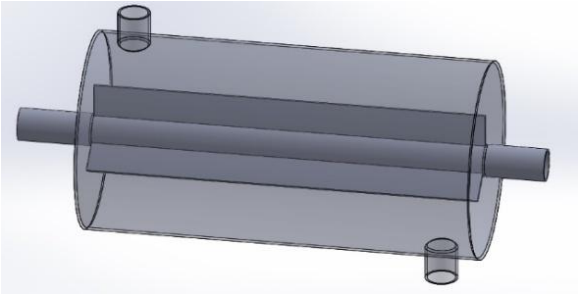

Fig 4.Transperent model of heat exchanger

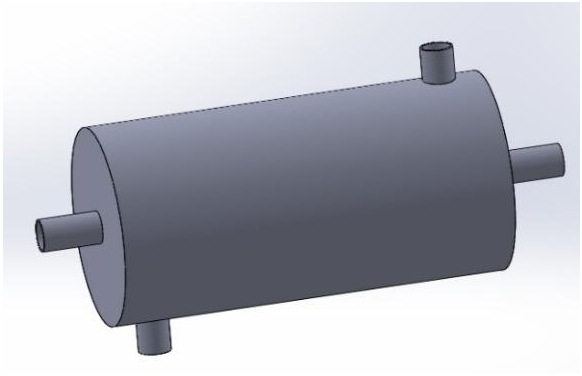

Fig 5.Original model of heat exchanger

TABLE.1. Dimensions of various parts of Heat exchanger.

Sl.No.	Component	Dimension	Quantity
01	Outer pipe (Air flow)	Length = 60 cm Diameter = 30 cm Thickness = 0.2 cm	01
02	Fins (Rectangular)	Length = 50 cm Height = 5 cm Thickness = 0.3 cm	03
03	Fins (Triangular)	Base =0.3cm Height = 5 cm	03
04	Inner pipe (Exhaust gas flow)	Length = 60 cm Diameter = 3.81 cm	01

TABLE.2 Thermal properties of mild steel, air and exhaust.

	$\rho(kg/m^3)$	C_p (J/kg K)	μ(kg/m s)	k(W/mK)
Air	1.225	1.006	1.789×10^{-5}	0.0242
Exhaust gases	0.8322	1016.8	2.384×10^{-5}	0.035
Mild steel	7850	510.78	-	64.875

Meshing

The meshing of heat exchanger is shown in Fig.6. The below Fig. 6(a) shows the mesh over the whole domain and Fig. 6(b) and Fig. 6(c) shows the inlet and outlet sectional views respectively.

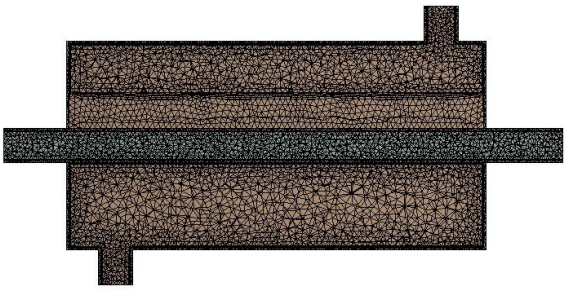

Fig 6. Total Domain mesh

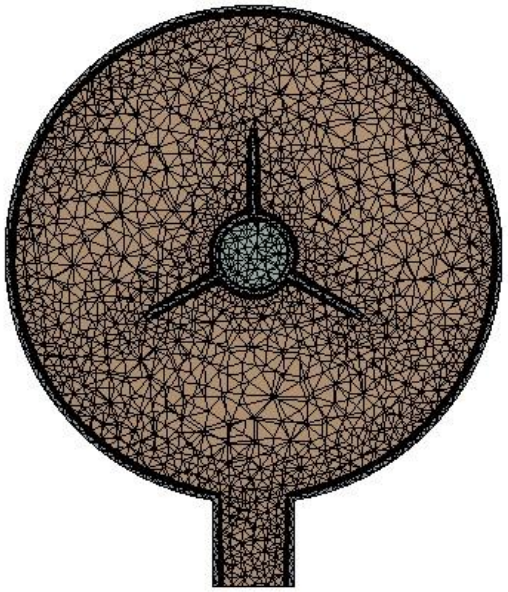

Fig (b).Inlet section mesh

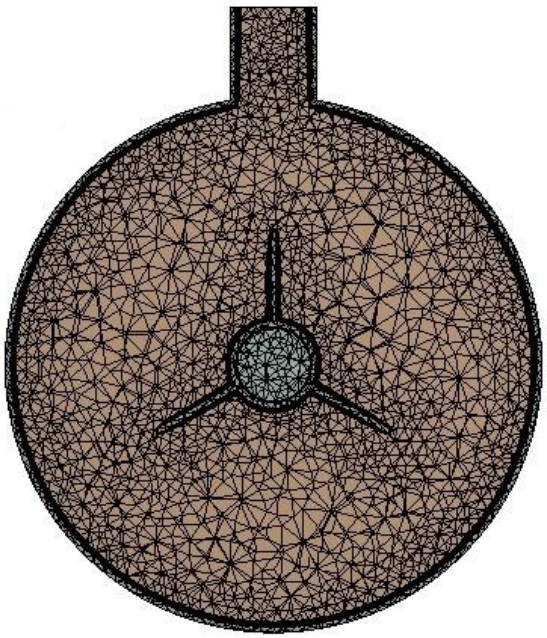

Fig (c).Outlet section mesh

Fig. 6. Meshing of Heat Exchanger

Temperature Contours

The temperature contour for 0%, 50% and 100% load are shown below in Figure 7, 8 and 9 respectively.

For 0% load

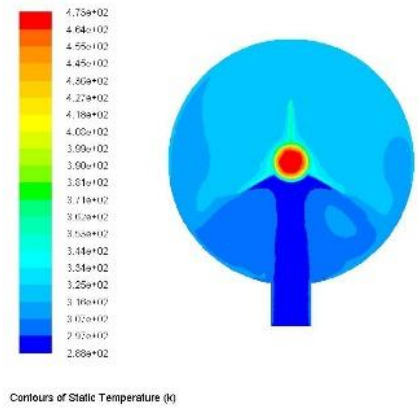

(a) Inlet Section

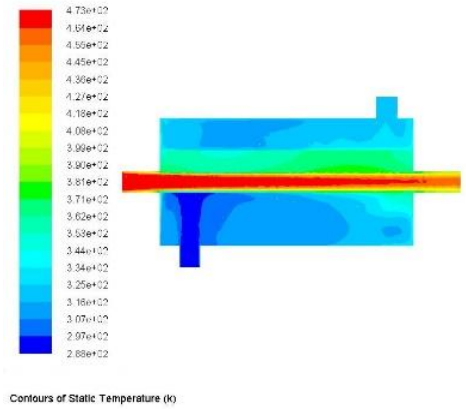

(b)Total section

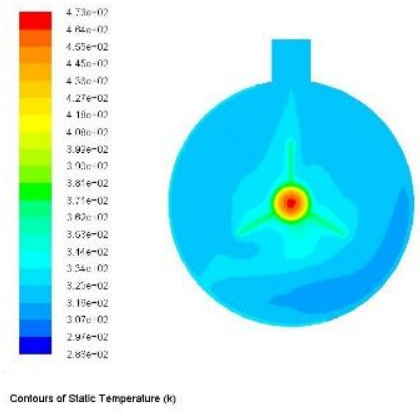

(c)Outlet Section

Fig 7. Temperature distribution of heat exchanger.

For 50% load

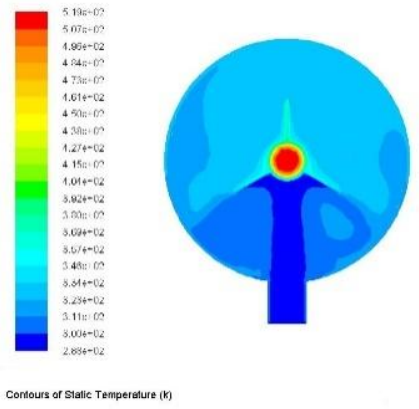

(a) Inlet Section

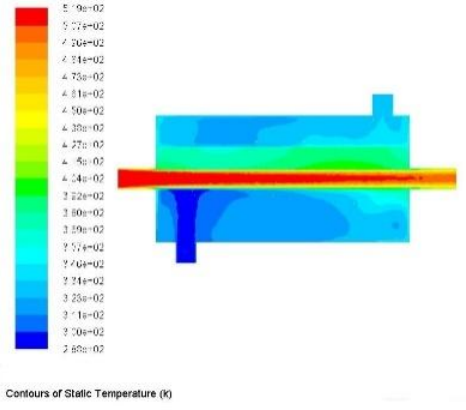

(b)Total section

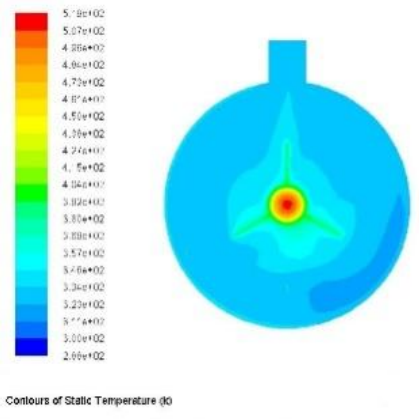

(c)Outlet Section

Fig. 8. Temperature distribution of heat exchanger.

For 100% load

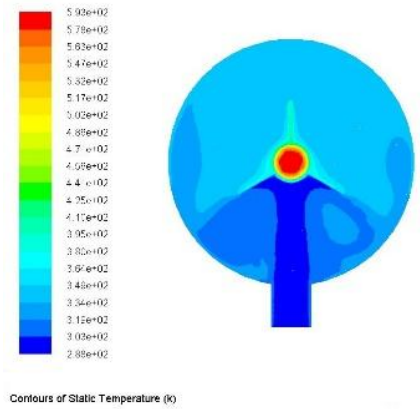

(a) Inlet Section

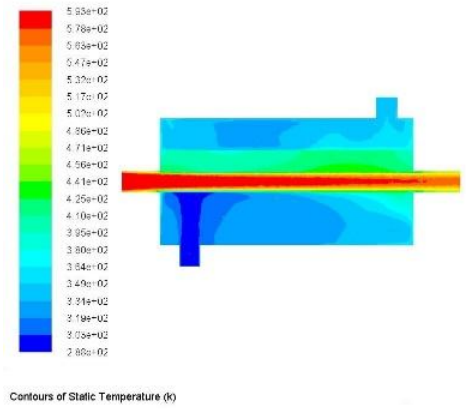

(b)Total section

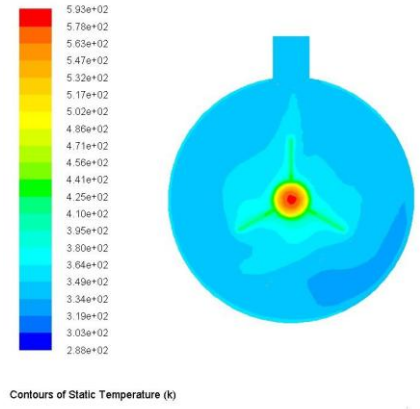

(c)Outlet Section

Fig. 9. Temperature distribution of heat exchanger.

Results and discussion

Performance of heat exchanger when it act as an air preheater

Initially engine was started and then air is preheated by the help of air pre-heater using heat energy of exhaust gas during cold weather condition. Then the experiment is conducted using preheated air for different loading conditions. During cold weather, at 15°C atmospheric temperature for preheating the engine inlet air, air from the air box is allowed to pass through the air pre-heater where it receives heat from the hot exhaust gas coming out of the engine. The readings for various parameters are recorded at different loads (0, 50 and 100%).

Engine exhaust temperature

Exhaust outlet temperature increases with increase in engine load due to slow evaporation of fuel constituents having higher boiling points burns in the late combustion phase. At different engine load the experimental engine exhaust temperature is shown in Fig. 10.

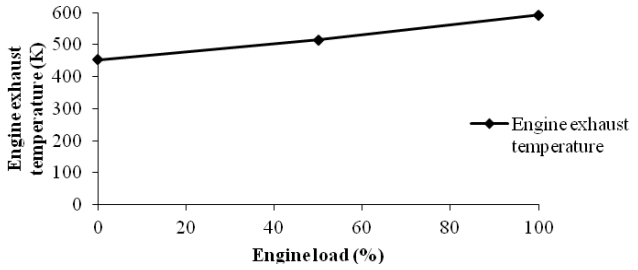

Fig.10 Variation of engine exhaust temperature with engine load.

Preheated air temperature at full opening of exhaust valve

Preheated air temperature increases with increase in engine load. The experimental preheated air temperature is found less compared to theoretical value. Result shows that at 100% engine load, the preheated air temperature for RNG and realizable simulation of rectangular and triangular fins are 389K, 372K, 397K and 384K respectively, which is 10.28%, 6.18%, 10.57% and 7.55% higher compared to experimental preheated air temperature using rectangular and triangular fins as shown Fig.11.

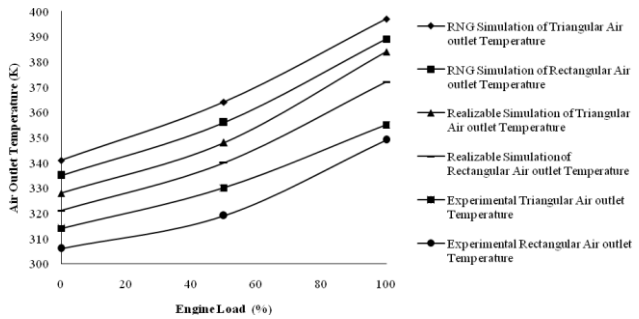

Fig.11 Variation of air outlet temperature with engine load.

Preheated air temperature at control exhaust flow rate

Preheated air temperature increases with the increase in mass flow rate of exhaust gas. Fig.12 & 13 shows the preheated air temperature of rectangular and triangular fins with different mass flow rate of exhaust gas.

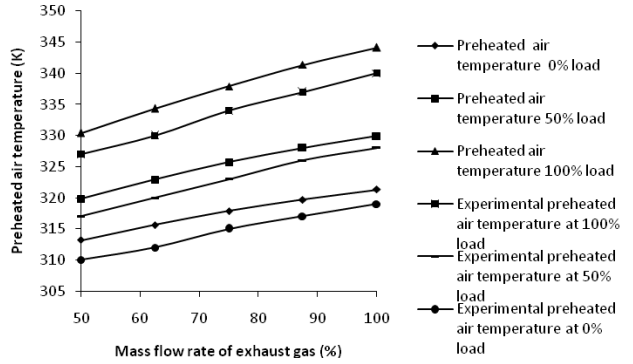

Fig.12 Variation of preheated air temperature of rectangular fins with the mass flow rate of exhaust gas.

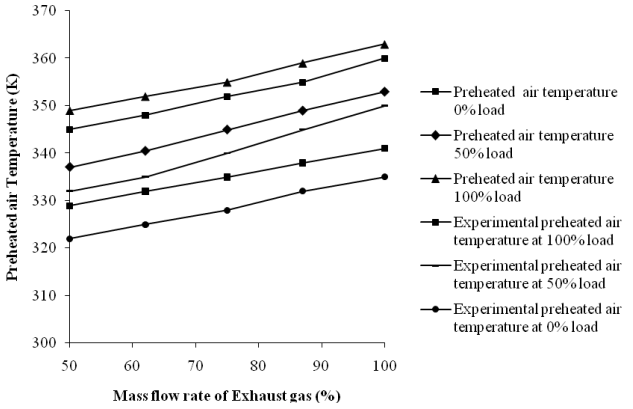

Fig.13 Variation of preheated air temperature of triangular fins with the mass flow rate of exhaust gas.

Performance of heat exchanger when it acts as a dryer

This heat exchanger can be used as a dryer for drying of different vegetables or products using different air flow rate of air. The performance of heat exchanger as a dryer is analysed at different atmospheric temperatures.

Preheated air temperature for drying at 273K atmospheric temperature

At low percentage of air mass flow rate the highest air outlet temperature is obtained. Fig.14-15 shows the increase in air outlet temperature at 273K inlet air temperature using rectangular and triangular fins with engine load. When inlet air temperature increases then air outlet temperature also increases for all air mass flow rate. At 100% engine load and 60% air mass flow rate of air, air outlet temperatures are found to be 356.14K, 359.84K, 363.54K and 367.24K when air inlet temperatures are kept 273K, 278K, 283K and 288K respectively using rectangular fins.

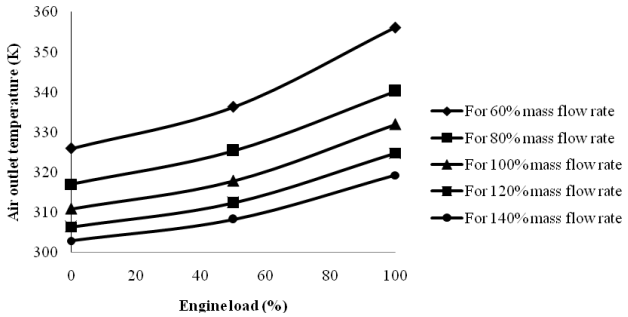

Fig.14 Preheated air temperature when atmospheric temperature is at 273K using rectangular fin.

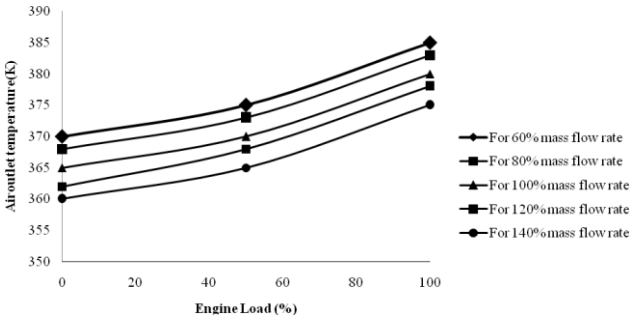

Fig.15 Preheated air temperature when atmospheric temperature is at 273K using triangular fin.

Engine performance, combustion and emission analysis

Initially engine is started and experimented during cold weather condition when atmospheric temperature is at 15°C. Then the air is preheated by the help of air preheater using heat energy of exhaust gas during cold weather condition. Using preheated air again the engine is experimented and analysed.

Brake specific fuel consumption (BSFC)

Brake specific fuel consumption decreases with increase in load. With pre-heated air, specific fuel consumption reduces. This may be referred to improved atomization of fuel at higher inlet air temperature leading to proper air fuel mixing and improved rate of combustion. The results obtained for BSFC at full load with air preheating and cold weather condition are found to be 0.31 Kg/kWh and 0.34 Kg/kWh respectively. The variation of BSFC with engine load is shown in Fig 16.

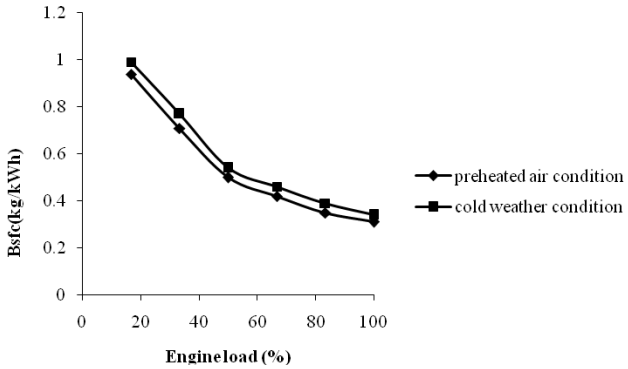

Fig.16 Variation of BSFC with engine load

Brake thermal efficiency (BTE)

BTE increases with increase in load as shown in Fig. 17. The improvement in BTE is more significant at higher brake outputs which are observed at higher loads. It may be due to higher in-cylinder temperature which improves vaporization of the fuel. Using preheated air makes a significant improvement in thermal efficiency may be due to better atomization and combustion. Brake thermal efficiency increases by 2.61% during air preheating compared to cold weather condition in full load condition.

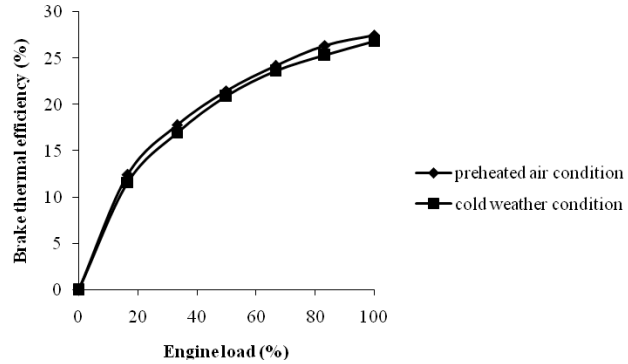

Fig.17 Variation of BTE with engine load

Cylinder pressure

Using preheated air the variation of cylinder pressure with crank angle is shown in Fig.18. Preheated air makes a significant improvement in cylinder pressure may be due to better atomization, mixing which improves combustion. Preheated air gives maximum cylinder pressure as compared to cold weather condition. Cylinder pressure increases by 0.8% using preheated air compared to cold weather condition.

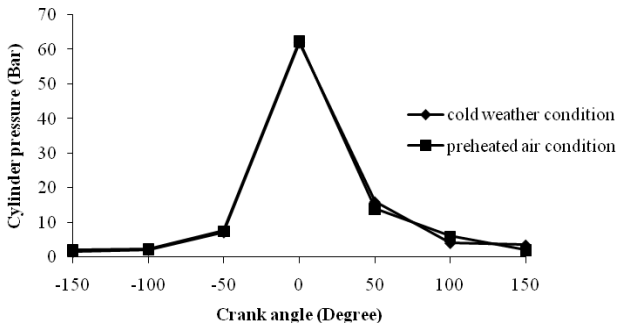

Fig. 18 Variation of Cylinder pressure with crank angle

Carbon Monoxide (CO)

CO emission decreases with increase in load as shown in Fig 18. The CO emission in cold weather condition is found higher compared to preheated air condition because of incomplete combustion of fuel at lower temperature. This may be due to better atomisation and mixing of fuel which leads to better combustion using preheated air.

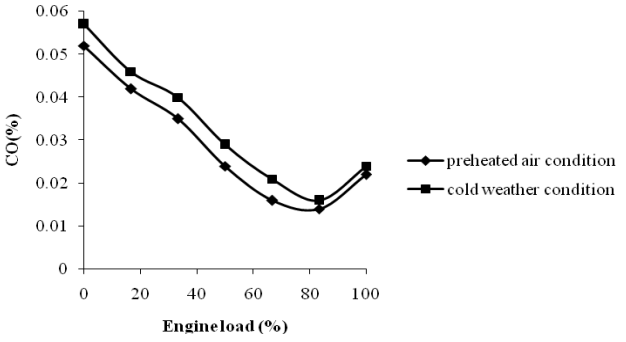

Fig 18 Variation of carbon monoxide with engine load

Hydrocarbon (HC)

HC emission using preheated air decreases as shown in Fig 19. The decrease in emission may be due to better combustion for higher inlet air temperature. The result shows HC emission during air preheating reduced by 5.46% at full load compared to cold weather condition.

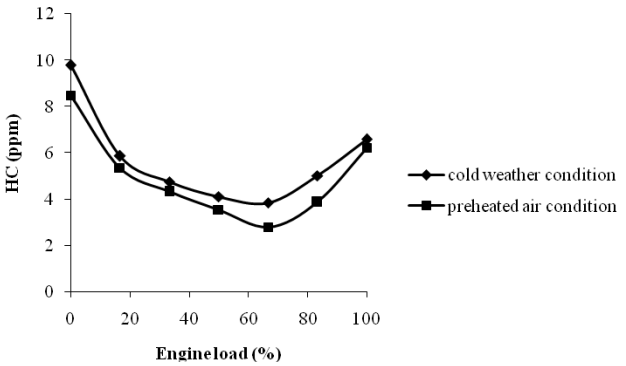

Fig 19 Variation of Hydrocarbon with engine load

Nitrogen oxide (NO)

Using preheated air NO emission increases with increase in load as shown in Fig. 20. This may be due higher combustion temperature developed using preheated air. NO emissions at full load are found to be higher by 10.83% during air pre-heating compared to cold weather condition.

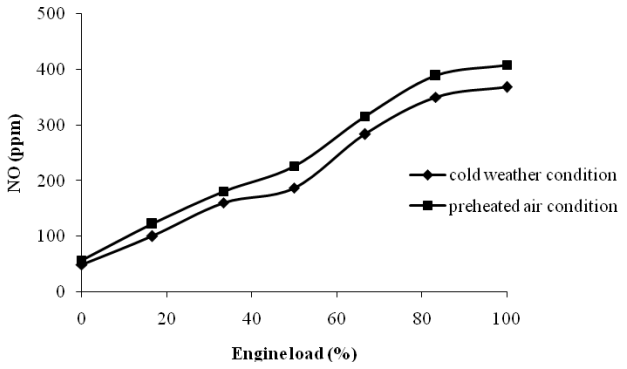

Fig 20 Variation of nitrogen oxides with engine load

Smoke Opacity

Fig 21 shows the variation of smoke opacity with different loads. Using preheated air smoke opacity is found to be decreased compared to cold weather condition. This may be due to better mixing of fuel at higher inlet air temperature which leads to better combustion of fuel during preheating. At full load smoke opacity is found 3% higher compared to their cold weather condition using preheated air.

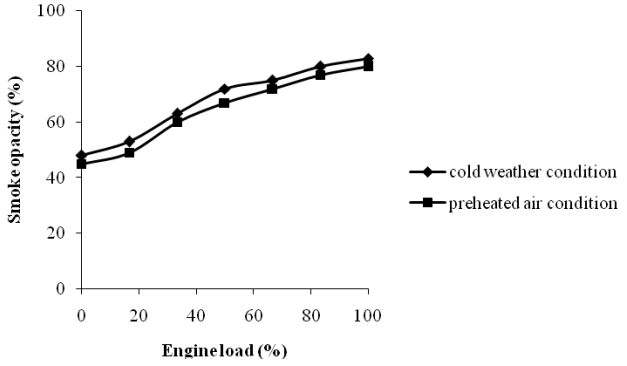

Fig 21 Variation of Smoke opacity with engine load

Conclusion

A finned tube heat exchanger with rectangular and triangular fin was analysed and compared using CFD and experimental results. Both the results are validated. From the results it found that triangular fins have better results as compared to rectangular fins.

The performance, combustion and emission characteristics of a CI engine with diesel have been investigated at cold weather condition and compared with preheated air condition. Following characteristics are concluded:

- BSFC decreases with increase in load during air preheating. Brake specific fuel consumption decreases by 8.82% using preheated air compared to cold weather condition.
- BTE increases with increase in load. Brake thermal efficiency increases by 2.61% using preheated air compared to their cold weather condition.
- The CO emission decreases by 8.33% using preheated air compared to cold weather condition.
- The HC emission decreases by 5.46% using preheated air compared to cold weather condition.
- The smoke opacity decreases by 10.2% using preheated air compared to cold weather condition.

References

[1] R. Saidur, N.A. Rahim, H.W. Ping, M.I. Jahirul, S. Mekhilef, and H.H. Masjuki, "Energy and emission analysis for industrial motors in Malaysia," Eng Pol., vol. 37, no. 9, pp. 3650-3658, 2009.

[2] M. Hatami, D.D. Ganji, and M.G. Bandpy, "A review of different heat exchangers designs for increasing the diesel exhaust waste heat recovery," Renew. Sust. Energy Rev, vol. 37, pp. 168-181, 2014.

[3] M. Ghazikhani, M. Hatami, and B. Safari,"The effect of alcoholic fuel additives on exergy parameters and emissions in a two stroke gasoline engine, "Arabian. J. Sci. Eng, vol. 39, no. 3, pp. 2117-2125, 2014.

[4] M. Ghazikhani, M. Hatami, and B. Safari, "Effect of speed and load on exergy recovery in a water cooled two stroke gasoline-ethanol engine for the bsfc reduction purposes," Sci Iranica, vol. 21, no. 1, pp. 171-180, 2014.

[5] S. Bari, and S. N. Hossain, "Waste heat recovery from a diesel engine using shell and tube heat Exchanger," App The Eng, vol. 61, pp. 355-363, 2013.

[6] Q. Wang, Q Chen, G. Chen, and M. Zeng, "Numerical investigation on combined multiple shell-pass shell-and-tube heat exchanger with continuous helical baffles," Int J of Heat and Mass Transfer, vol. 52, pp. 1214–1222, 2009.

[7] B. Drobnic, J. Oman, and M. Tuma, "A numerical model for the analyses of heat transfer and leakages in a rotary air preheater," Int J of Heat and Mass Transfer, vol. 49, pp. 5001–5009, 2006.

[8] M. Zeng, L.X. Du, D. Liao, W.X. Chu, Q.W. Wang, Y. Luo, and Y. Sun, "Investigation on pressure drop and heat transfer performances of plate-fin iron air preheater unit with experimental and Genetic Algorithm methods," App Eng, vol. 92, pp. 725–732, 2012.

[9] Ting Ma, Q.W.Wang, M. Zeng, Y.T.Chen, Y.Liu, & V.Nagarajan., "Study on heat transfer and pressure drop performances of ribbed channelin the high temperature heat exchanger," App Eng, vol. 99, pp. 393–401, 2012.

[10] M. Hatami, and D.D. Ganji, "Thermal performance of circular convective–radiative porous fins with different section shapes and materials," Eng Conv and Mag, vol. 76, pp. 185–193, 2013.

[11] H. Bilirgen, S. Dunbar, and E.K..Levy, "Numerical modeling of finned heat exchanger," Applied thermal Engineering, vol. 61, pp. 278–288, 2013.

[12] Juan. Li, Xiang. Ling, and Hao. Peng, "Field synergy analysis on convective heat transfer and fluid flow of a novel triangular perforated fin," Int Jour of Heat and Mass Transfer, vol. 64, pp. 526–535, 2013.

[13] M. Turkyilmazoglu, "Stretching/shrinking longitudinal fins of rectangular profile and heat transfer," Eng Conv and Mang, vol. 91, pp. 199–203, 2015.

[14] Zhen-Xing. Li, Ting-Shu. Zhong, Jian-Lei. Niu, Fu. Xiao, and Li-Zhi. Zhang, "Conjugate heat and mass transfer in a total heat exchanger with cross-corrugated triangular ducts and one-step made asymmetric membranes," Int Jour of Heat and Mass Transfer, vol. 84, pp. 390–400, 2015.

[15] Hamidreza. Shabgard, Michael J. Allen, Nourouddin. Sharifi, Steven P. Benn, Amir. Faghri, and Theodore L. Bergman,"Heat pipe heat exchangers and heat sinks: Opportunities, challenges, applications, analysis, and state of the art," Int Jour of Heat and Mass Transfer, vol. 89, pp. 138–158, 2015.

[16] Hasan, and M. Ismael., "Investigation of flow and heat transfer characteristics in micro pin fin heat sink with nanofluid," App Ther Eng, vol. 63, pp.598-607, 2014.

[17] Ting. b. Maa, Qiu-wang. Wang, Min. a. Zeng,, Chen, Yi-tung. B., Liu Yang b., and Vijaisri. Nagarajan, "Study on heat transfer and pressure drop performances of ribbed channel in the high temperature heat exchanger," App Eng, 99, pp. 393–401, 2012.